On the Relationship Between Deformation-Induced Surface Roughness and Plastic Strain in AA5052—Is it Really Linear?

M.R. STOUDT, J.B. HUBBARD, and S.D. LEIGH

Three different heat treatments of aluminum alloy AA5052 were subjected to various levels of uniaxial plastic strain. The resulting surfaces were then evaluated using both scanning laser confocal microscopy (SLCM) and stylus profilometry. Three regression approaches were used to assess the quality of a linear and a curvilinear fit for the roughness data as a function of true plastic strain. While there were differences among the regression results, the analyses revealed that a linear model was more statistically appropriate for the finest grain size. As the grain size increased, the surface morphology became more complex and a quadratic model became more suitable. Since the relative area fractions of grain boundary–localized roughness and slip-induced roughness are grain size dependent, the higher order fit between the roughness and plastic strain reflects substantial changes in the ratio of these areas. The differences between the SLCM and profilometry results were attributed to the natural filtering that occurs during contact profilometry. This filtering skewed the roughness data toward the largest surface displacements, thereby reducing the measurement fidelity to the point where the only possible outcome was the linear relationship.

I. INTRODUCTION

DISCREPANCIES between measured surface roughness values and those predicted by numerical modeling call into question the reliability of the material property data used by models that predict the mechanical behavior. While this article focuses on the reliability of the mechanical property data in sheet metal formability models, such inconsistencies can also affect the accuracy of computational models for material design.[1,2] More specifically, the fact that discrepancies exist implies either that the current approaches for acquiring and analyzing deformation-induced surface roughness are not appropriate for the task or that the measured data lack sufficient measurement fidelity. Undoubtedly, the accuracy of any surface roughness evaluation strongly depends on the technique used to acquire the topographic data, and while all surface measurement methods introduce error to some extent, careful examination of the characteristics of these errors have established appropriate measures for correction.[3,4] When performed properly, most surface characterization techniques provide sufficient measurement resolution, so the more likely source of discrepancy is the manner in which the surface data are assessed. Many of the assessments of roughening behavior reported in the literature are derived from sets of linear profiles and use time series–based statistical sampling protocols to evaluate the roughness data.[5] These assessments typically express the surface roughness as the simple average of a scalar roughness parameter that describes the dispersion about the profile mean (e.g., the arithmetic mean roughness, Ra, or the root-mean-squared roughness, Rq). This averaged mean roughness parameter is then typically extrapolated to represent the characteristics of the entire surface at a given particular strain level (i.e., a surface-Ra or a surface-Rq value). The key factor is that the surfaces are assumed to have a statistically stationary form (i.e., the statistical properties are invariant with respect to translation in position on the surface), because stationarity is a requirement if the extrapolation is to have any meaning. There are two fundamental problems with this approach: (1) the commonly used scalar parameters do not sufficiently account for the complexity of the deformation in a polycrystalline material[6,7] and (2) extrapolation will compound any measurement uncertainty or statistical errors present in the roughness data. For these reasons, representations of the surface character derived from surface roughness data of this type could easily over simplify the true behavior and produce misleading results. The high likelihood for error in these surface roughness analyses raises questions about the validity of the linear relationship presumed between deformation-induced roughness of a free polycrystalline surface and plastic strain that prevails in the surface roughness literature.[8–13] The literature also indicates that when the complexities in the deformation process are properly considered, such as in the molecular dynamic simulation results reported by Perron et al.,[14] the relationship between the computed surface roughness and strain is distinctly nonlinear.

M.R. STOUDT, Research Engineer, and J.B. HUBBARD, Guest Researcher, are with the Material Measurement Laboratory, NIST Center for Automotive Lightweighting, National Institute of Standards and Technology, Gaithersburg, MD 20899-8553. Contact e-mail: stoudt@nist.gov S.D. LEIGH, Statistician, is with the Statistical Engineering Division, Information Technology Laboratory, National Institute of Standards and Technology.
Manuscript submitted March 11, 2010.
Article published online April 29, 2011

A recent study evaluated the nature of the relationship between surface roughness and plastic strain in AA6111-T4 aluminum using surface roughness data acquired with scanning laser confocal microscopy (SLCM) and two different analysis protocols.[15] The first protocol was consistent with the method reported in the literature in that a surface-Rq value was determined from sets of widely spaced linear roughness profiles. Specifically, each profile data set consisted of eight regularly spaced columns that were extracted from numerical matrices of topographical data acquired at the different strain conditions. The second protocol determined the surface-Rq value (Sq) with a single calculation that included all the data points within the same numerical matrix. When the surface data derived from the two different protocols were plotted against plastic strain, the large uncertainties associated with the first protocol (*i.e.*, the profile-based approach) produced a linear correlation coefficient of 0.95, which would seem to indicate an excellent overall fit. However, the data from the second protocol exhibited a distinctly nonlinear form that clearly did not support the literature consensus of a universal linear relationship, because the associated uncertainties in the data were minimized by the matrix-based calculation. Further analysis of these results revealed that when a surface-Rq value is derived from a set of individual profiles, it is highly influenced by the sampling conditions and by the presence of the natural correlations that exist within the profile data. In contrast, when Sq is obtained from a single matrix-based calculation, any influence arising from correlations within the roughness data is eliminated. In fact, after the correlations in the profile data were eliminated, the same data produced a nonlinear behavior that was nearly identical to that exhibited by the matrix-based Sq data. There were two main conclusions drawn from this study. The approach used to interpret the roughness data as independent profiles does not accurately represent the true roughening behavior of the free surface of a polycrystalline material even though the correlation statistics may suggest an excellent fit, and the linear relationship between Rq and plastic strain reported in the literature is a statistical artifact resulting from inadequate sampling.

In 2002, Stoudt and Ricker[7] reported that height-based mean roughness parameters that reduce a roughness profile to a single value, such as Ra, may adequately quantify the macroscopic changes that occur on a surface with plastic strain in a commercial, polycrystalline aluminum alloy. In light of the findings in Reference 15 and the citations of Reference 7 supporting claims of a universal linear relationship between surface roughness and plastic strain,[16,17] it is appropriate to re-evaluate the conclusions reported by Stoudt and Ricker. As such, this article compares roughness data of uniaxially strained AA5052 that were acquired with contact profilometry to data from the same set of surfaces that were acquired by SLCM. The approach used to evaluate these data is similar to the one used in Reference 15, with the key distinction being that the profile data is actual profilometer data. That is, the profile data were not extracted from a matrix. For this

reason, many of the issues associated with stylus profilometry such as filtering and mechanical damage are relevant here, whereas they were inconsequential in Reference 15.

II. EXPERIMENTAL

A. *Material*

As described in Reference 7, aluminum alloy AA5052 has a nominal Mg mass fraction of 2.5 pct and an approximate Cr mass fraction of 0.25 pct to control grain size and to enhance strength.[18] Three heat treatments were developed to create different grain sizes: (1) 96 hours at 813 K (540 °C) (hereafter referred to as the HT condition); (2) 2 hours at 623 K (350 °C) (hereafter referred to as the O condition); and (3) the as-received, or H32 condition. The designation H3x refers to a stabilized condition produced through a low-temperature thermal treatment designed to retain a small amount of the residual strain to stabilize the mechanical properties and the ductility.[18] The grain size was measured in each heat-treated condition in both the rolling direction (RD) and the long transverse direction (TD) using a linear-intercept technique similar to that prescribed in ASTM Standard E-112.[19] The grain size data, as reported by Stoudt and Ricker,[7] are shown in Table I.

B. *Generation of Surface Roughness*

Flat sheet, tensile specimens were machined from 1.0-mm-thick sheet stock with the tensile axis oriented parallel to the RD. All of the specimens in this analysis were obtained from the same sheet to minimize variations in the crystallographic texture and the heat treatment.

Sample preparation consisted of polishing the entire specimen surface to a 0.25-μm diamond finish using standard metallographic practice.[20] A grid of fiducial lines spaced nominally at 5-mm intervals was lightly engraved on the gage section of each specimen with a silicon carbide scribe to facilitate assessment of the local plastic strain. The initial spacing between the lines on the grid was determined with a linear-encoded, measuring stage microscope with a resolution of ±0.5 μm. The specimens were pulled in uniaxial tension to predetermined levels of plastic strain with a computer-controlled universal tensile machine. The crosshead displacement rate was 1.5 mm/s for all experiments. After the desired strain level was attained, the grid was remeasured with the microscope and the true plastic strain was calculated

Table I. Analysis of the Grain Size

Heat Treatment	Grain Size (RD) (μm)	Standard Error (μm)	Grain Size (TD) (μm)	Standard Error (μm)	Aspect Ratio (LT/RD)
H32	53.48	1.42	51.51	0.67	1.092
O	134.52	4.65	124.64	8.53	1.079
HT	159.31	7.66	154.63	6.37	1.030

Table II. Analysis of the Error in Strain			
Heat Treatment	True Strain	Standard Uncertainty (σ)	Relative Standard Uncertainty of Mean (Pct)
H32	0	0	0
H32	0.0362	0.0048	0.0469
H32	0.0486	0.0020	0.0164
H32	0.0889	0.0030	0.0146
H32	0.0946	0.0065	0.0264
O	0	0	0
O	0.0424	0.0022	0.0165
O	0.0778	0.0058	0.0283
O	0.0919	0.0008	0.0033
O	0.1226	0.0046	0.0139
O	0.1658	0.0068	0.0169
O	0.1796	0.0078	0.0162
O	0.1994	0.0068	0.0140
HT	0	0	0
HT	0.0286	0.0006	0.0105
HT	0.0449	0.0005	0.0045
HT	0.0905	0.0045	0.0210
HT	0.1082	0.0012	0.0046
HT	0.1326	0.0131	0.0053
HT	0.1415	0.0014	0.0375

from the grid displacement. The true strain values shown in Table II differ slightly from those originally reported in Reference 7, because the strain data were evaluated more comprehensively for this study. The recomputed strain values and the associated error are shown in Table II.

C. Contact Profilometry

Some of the samples used to generate the data shown in Reference 7 were re-strained to higher strain levels and could not be re-evaluated. As such, the set of strain levels is smaller for this analysis than what was originally reported.

The first method used to acquire surface data was contact profilometry.[7] For these measurements, roughness profiles were acquired in the region of the specimen where the plastic strain level was closest to the target value. Each surface measurement consisted of five 1.75-mm profiles made with a 5-μm-diameter stylus in both the RD and TD orientations to generate ten profiles in total. A space of approximately 1.0 mm was left between profiles along the grid section to ensure that there was no overlap. Each profile consisted of 8064 data points, which created a sampling interval of approximately 0.22 μm/point. Each profile was corrected for offset effects resulting from specimen tilt or other mechanical influences by computing the optimal regression equation of the profile and then subtracting the regression from each point in the image matrix.

D. Scanning Laser Confocal Microscopy

The second method acquired surface data by SLCM. Each surface measurement consisted of five, well-spaced SLCM topography images taken from the center region of the specimen. All of the SLCM images were created with a 635-nm red laser source. For each image, the spacing between sampling points in the (x, y) plane was fixed by the objective lens at 1.562 μm/point, and the spacing between the individual focal planes in the z direction was nominally 100 nm. These sampling parameters generated sets of (640 $\times$ 512) pixel images with physical dimensions (x,y,z) of (1000 $\times$ 800 $\times$ $\approx$50) μm. As with the profile data, it was essential that these images be well separated to ensure that the surface data contained in each image were uncorrelated (*i.e.*, no overlapping of any image data) and that the data properly represented the full range of surface characteristics. The specifics of the procedure to convert the SLCM images to simple matrices of topographic heights are described in Reference 15. After conversion, the numerical matrices were trimmed to square 262,144 element arrays (*i.e.*, 512 pixels $\times$ 512 pixels) to facilitate the matrix-based mathematical operations. Each matrix was leveled using a similar procedure to that used to minimize offset effects in the profile data. In this case, the optimal multiple regression equation of the Euclidean plane was computed for each matrix and was then subtracted from each point in the image matrix.

Because some of the statistical parameters used to interpret the surface data are highly sensitive to outliers, the extreme values were filtered from all of the profilometer and SLCM data sets. For this evaluation, an extreme value was defined as any value that was greater than $\pm 6\sigma$, where σ is the standard deviation for all the heights in that particular data set. Filtering consisted of setting the magnitude of any data points that met this criterion equal to the mean for that particular data set. Note that the number of affected data points for a given data set was typically less than 20 points. The residuals were used as the source for all subsequent assessments of the surface character.

III. ANALYSIS METHODS AND RESULTS

A. Evaluation of Surface Roughness Data

The increasingly complex relationship between plastic strain and the evolved surface morphology is exhibited in Figure 1. The high-resolution intensity SLCM images in this figure illustrate how much the surface character changes at low, medium, and high strain levels in the O heat treatment.

Prior to evaluation, we merged the individual roughness measurements using a superposition technique. The superposed data were rank-sorted and binned into histograms that represented the entire surface height distributions for each heat treatment and strain condition. This technique was repeated to produce two complete sets of data from the same surfaces: one acquired by SLCM and one by contact profilometry.

Probability density functions (PDFs) were calculated from the histograms of the height data. As shown previously, raw topographic data have a character that can generally be described with Gaussian statistics.[6,15,21,22] This is convenient since Rq is defined as one standard deviation of the normal distribution

Tensile Direction

(a) 4.5 % TD RD

(b) 9.6 % TD RD

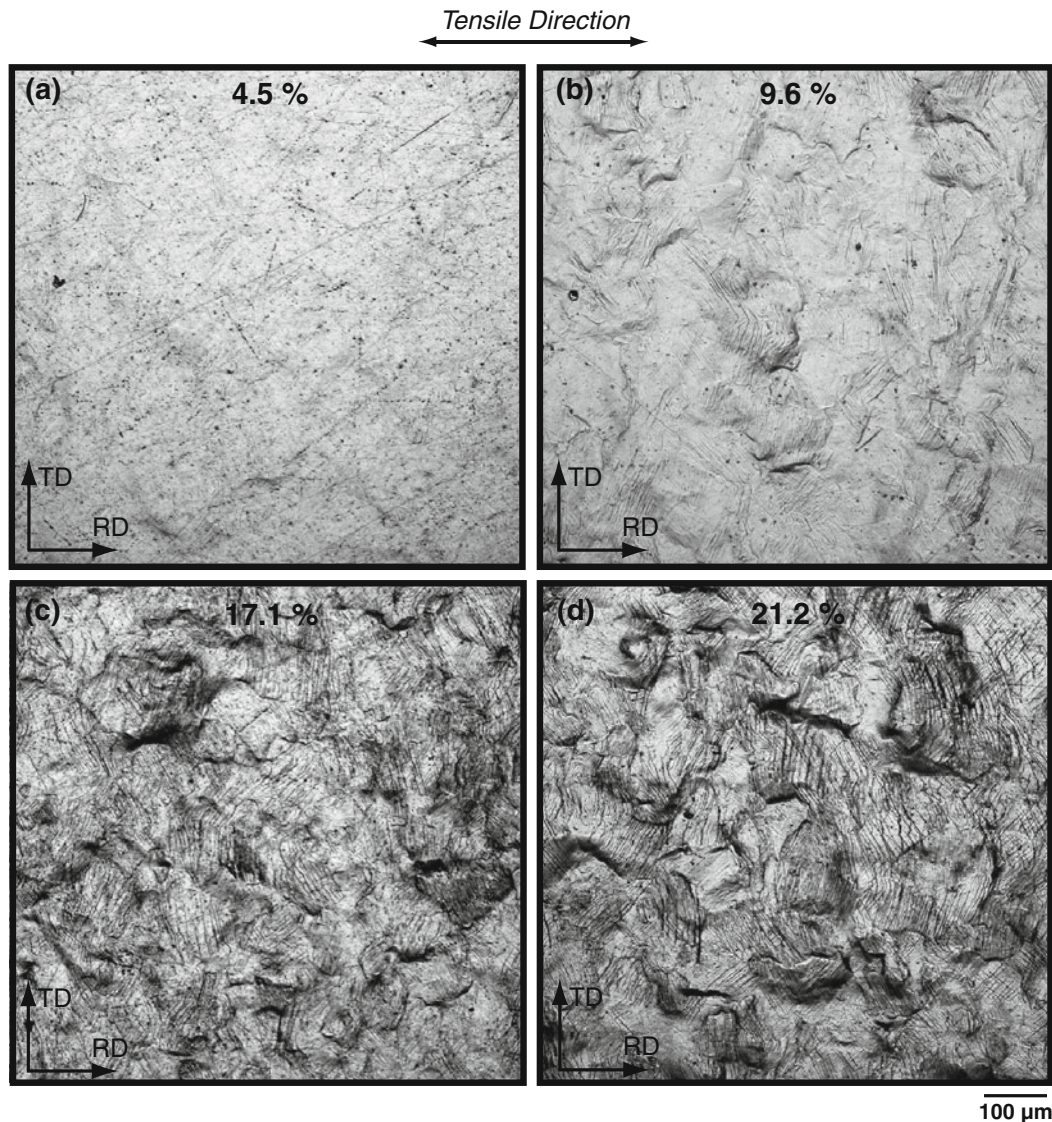(c) 17.1 % TD RD

(d) 21.2 % TD RD

100 μm

Fig. 1—A series of scanning laser confocal micrographs showing the progressive complexity of the relationship between plastic strain and the surface morphology of AA5052 in the O heat treatment. (*a*) The surface after the application of 0.045 true strain. (*b*) The surface after the application of 0.096 true strain. (*c*) The surface after the application of 0.171 true strain. (*d*) The surface after the application of 0.212 true strain.

(*i.e.*, $Rq \equiv \sigma$).[23,24] Even though it is more common in the surface roughness literature, Ra has no definitional association to the moments of the height distribution. Since the calculations here are based on the merged distribution, σ becomes an estimate of the Rq value for the entire surface, or Sq. The expression used to determine Sq is[23]

$$\mathrm{Sq} = \left[\left(\frac{1}{N} \right) \sum_{j=1}^{N} \left(Z_j - \overline{Z} \right)^2 \right]^{1/2} \qquad [1]$$

In this equation, Z is a set of height values, $\overline{Z}$ is the mean of Z, and N is the total number of values in the calculation. We added the subscripts "slcm" and "prof" to the Sq data to distinguish the surface data acquired

by confocal microscopy from those acquired by contact profilometry.

Figure 2 shows the relationship between Sq_{slcm} and true plastic strain for the three heat treatments. The profilometry data (Sq_{prof}) are presented in exactly the same fashion in Figure 3. As noted previously, the uncertainties associated with the Sq data in both figures were minimized by the analysis protocol, and as a result, the error bars for the Sq data are substantially smaller than the plot symbols. Dashed lines connect the raw Sq data to illustrate the changes in the surface roughness as a function of plastic strain for each heat treatment, and with the possible exception of HT in Figure 3, none of the heat treatments exhibits any obvious linear trend. This is the case for both the SLCM and the profilometry data.
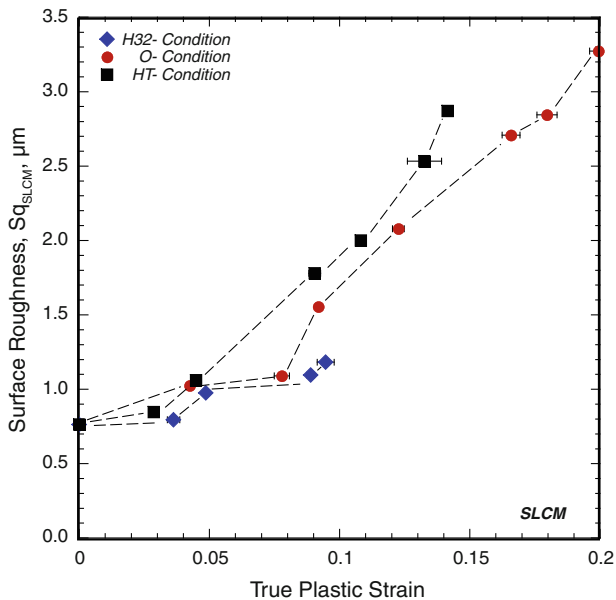
Fig. 2—The relationship between Sq and true plastic strain for the three heat treatments of AA5052. The surface data in this figure were acquired with scanning laser confocal microscopy. Note that the dashed lines connect the raw Sq data to illustrate the relative magnitude of the changes in the surface roughness as a function of plastic strain for each heat treatment. Because of the finer sampling conditions and higher density of data points, the behaviors shown in this figure are considered more representative of the actual relationships between Sq and plastic strain for the AA5052.
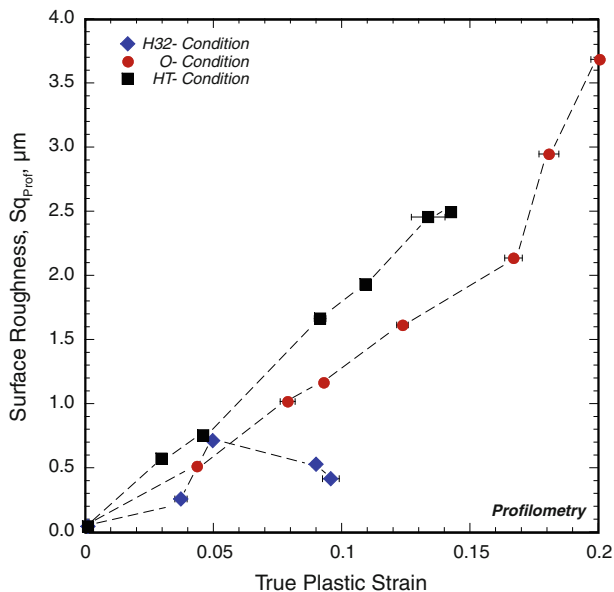

Fig. 3—The relationship between Sq and true plastic strain for the three heat treatments of AA5052. The surface data in this figure were acquired with contact profilometry. As in Fig. 2, the dashed lines connect the raw Sq data to illustrate the relative magnitude of the changes in the surface roughness as a function of plastic strain for each treatment.

One difference between the SLCM and profilometer data is the initial roughness at zero strain. As shown in Figures 2 and 3, the initial roughness is approximately 0.7 μm for the SLCM data, whereas the profilometer

value is considerably smaller at approximately 0.03 μm. Further examination shows that the offset between the SLCM and profilometer roughness data becomes negligible after the strain exceeds approximately 0.05. The slight shadowing visible in the topography of the as-polished, zero strain condition, shown in Figure 4(a), indicates that the difference in magnitudes is most likely due to a specular distortion resulting from the highly reflective surface in this condition. Since the variation in dispersion of the incident light generates the contrast, or signal, at each pixel point and the image is then created from that intensity map, imaging of flat, highly reflective surfaces with optical techniques is particularly difficult because these surfaces often reflect the incident laser with little or no dispersion. This tends to introduce anomalies in the surface measurement. The relatively small offset produced by this curvature artificially broadened the range of the height distributions from approximately ± 0.5 μm (profile) to approximately ± 4 μm (SLCM) and, consequently, increased the magnitude of Sq. This is reflected in the different shapes of the PDFs for the as-polished condition shown in Figure 4(b). Eliminating the curvature from linear profile data is relatively straightforward because the data are two-dimensional and the distortion only propagates in one measured dimension. However, eliminating the curvature from the SLCM data is more problematic, because the data are three-dimensional and distortions generally do not propagate symmetrically. The fact that correction measures are dependent on the length scale of the surface data involved and on the type of instrument used to acquire it[25] exacerbates the problem. That is, if the parameters used to correct for a distortion are inappropriate, the method will introduce additional distortions in the height data. Analyses of the different protocols reported in the literature to correct for form errors are outside the scope of this evaluation. We adopted the X-Y phase-correct Gaussian (PCG) high-pass filter protocol to correct the data, because it is the protocol recommended by the ASME Surface Roughness Standard B46[23] for form errors of this type. This protocol has been shown to effectively remove long wavelength two-dimensional distortions from three-dimensional data with minimum influence on the magnitude of the short wavelength (roughness) components.[26] After a series of parametric evaluations, we achieved the most effective filtering with a filter mask of 107.8 μm and a long wavelength cutoff of 34.4 μm. The change in the shape of the PDFs in Figure 4(c) shown before and after the application of the PCG filter demonstrates that the application of this high-pass filter considerably reduced the influence of the distortion. As shown in Figure 4(d), the influence of the distortion is strongest when the magnitude of the roughness is small. That is, the zero strain, as-polished surface condition has a poor signal-to-noise ratio. Furthermore, the convergence of the two lines in this figure indicates that as the magnitude of the roughness increases (signal), the relative influence of the distortion (noise) progressively diminishes to the point where the differences between the behaviors of the raw and filtered data are negligible. Based on the change exhibited in Figure 4(c), and the
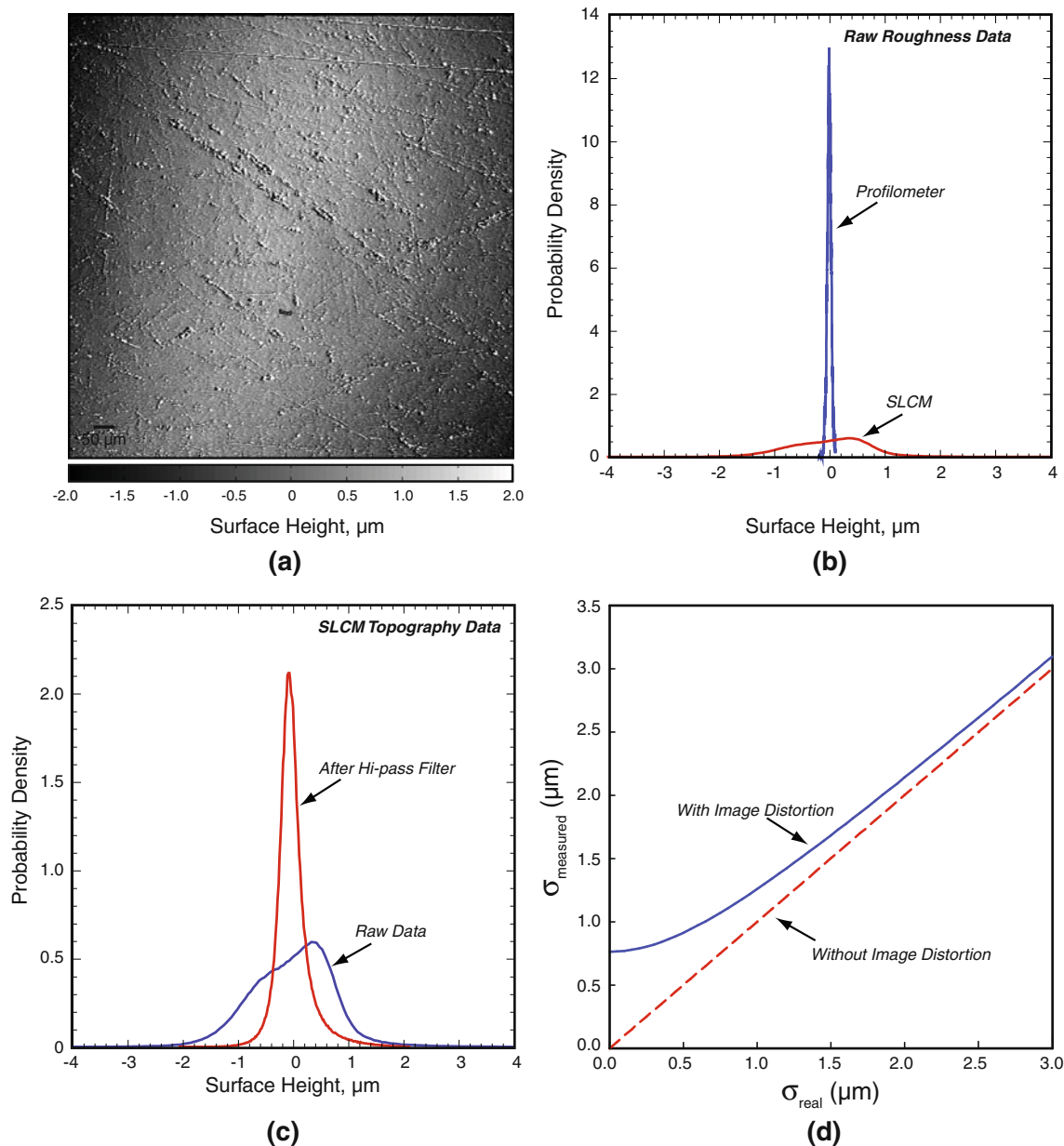
Fig. 4—The influence of specimen curvature on the height distribution. (*a*) A typical topography for the AA5052 in the as-polished/zero strain condition. (*b*) Probability distribution functions for the surface heights acquired by contact profilametry and by scanning laser confocal microscopy. (*c*) Probability distribution functions for the confocal data before and after a phase-correct Gaussian high-pass filter. (*d*) The behavior of the surface data with and without a small distortion.

fact that the distortion is not observable in any of the images shown in Figure 1, the difference between the profilometer and the SLCM height distributions was attributed to differences in the composition of the measured surface data and not to the influence of any form errors.

One objective of this study is to determine whether the relationship between plastic strain and surface roughness changes when the surface data are acquired by the SLCM. Considering that any filtering could influence the character of those relationships, and that the only SLCM data in this study that are appreciably affected by the distortion are those in the zero strain condition, we elected to compare both data sets in the same condition

(*i.e.*, flattened with a best regression fit). This decision was based on an additional analytical objective: to assess the trends in the behavior without introducing any additional bias.

B. Evaluation of the Statistical Model

The data available here for a statistical comparison of the goodness-of-fit between a straight-line model and a curvilinear model are derived from a limited number of strain states. In light of this, the curvilinear alternative to the linear model will be a simple quadratic expression. The formulas used for the statistical comparison to assess linearity are

$$Sq = A_0 + A_1\varepsilon \qquad [2]$$

$$Sq = A_0 + A_1\varepsilon + A_2\varepsilon^2 \qquad [3]$$

The objective of this analysis is to compare the quality of a simple linear fit (Eq. [2]) to a simple curvilinear fit (Eq. [3]) of Sq as a function of the true plastic strain, ε. Several approaches are suitable for this purpose; however, considering the limited range of the data, and the fact that both the line and the quadratic are linear in the coefficients, a standard analysis of variance (ANOVA) model comparison is a straightforward method to indicate the more appropriate fit.[27]

An F-test can be used to compare the performance of any pair of nested multilinear (or polynomial) models on a given data set. A quadratic model is an extension of a linear model in that it consists of a linear model with an additional term. As shown in Eq. [4], the F-test refers to the ratio of the residual sum of squares (RSS) of the partial linear model, minus the RSS of the full quadratic model, divided by the full model RSS normalized by appropriate degrees of freedom ($n - 3$) to the corresponding F distribution:[28]

$$F_{n-3} = \frac{\left(RSS_{linear} - RSS_{quadratic}\right)}{\left(\frac{RSS_{quadratic}}{n-3}\right)} \qquad [4]$$

The t-values associated with the coefficients of Eqs. [2] and [3] are shown for the SLCM data in Table III and for the profile data in Table IV. In general, a value ≥ 2.0 for any individual t-value indicates a statistically significant nonzero coefficient within a 95 pct confidence level (as defined by the Student's-t distribution[29]). As shown in Table III, all of the t-values are ≥ 2.0 for the linear

model, which suggests a credible linear trend with strain. However, the A_2 t-values for the O and HT conditions are also ≥ 2.0. This suggests that the data from these heat treatments could be quadratic as the linear terms are not distinguishable from zero ($t < 2$). In contrast, the t-values from the profile data (Table IV) do not indicate that either model is consistently applicable for any heat treatment. As such, the results from the simplest regression analysis are inconclusive.

Table V summarizes the ANOVA model comparisons. The data were assessed using the analysis of variance (ANOVA) model comparison, which is embedded in many standard statistical analysis packages for multilinear and polynomial fitting. This analysis used the built-in "model ANOVA" command in the software package S-plus* to perform the linear-quadratic com-

---

*Certain commercial equipment, instruments, or materials are identified in this article to foster understanding. Such identification does not imply recommendation or endorsement by the National Institute of Standards and Technology, nor does it imply that the materials or equipment identified are necessarily the best available for the purpose.

---

parisons on each of the Sq-strain curves under the two different (operating) regimes discussed here.[30] The small P-values in the table (<0.05) support rejection of the linear model (the null hypothesis) and acceptance of the quadratic model. In the case of the Sq_{slcm} data, the results shown in Table V establish that the linear fit is the statistically more appropriate fit for the H32 condition, whereas the quadratic fit is statistically more appropriate for the O and for the HT conditions. In fact, the P-value of 0.004 for the HT data strongly supports a preference for the quadratic model for this grain size. However, the results for the Sq_{prof} data do not indicate any significant improvement with a quadratic fit—with the O condition being the possible exception, where the P-value of 0.047 is ≈ 0.05.

There is a fundamental, but often overlooked assumption invoked with use of ordinary least squares (OLS) regression. That is, by using OLS to fit the expression $Y = f(X)$, one implicitly assumes that there is no error in the X variable (strain) and all the error is in the Y variable (Sq). Since most scientific measurements incur error in both the X and Y values, standard OLS methodology is generally considered applicable only if

Table III.   Analysis of the SLCM-Based Sq Data

Heat Treatment	Linear Model t-Values		Quadratic Model t-Values		
	A0 (Intercept)	A1	A0 (Intercept)	A1	A2
H32	13.450	5.279	10.780	0.589	0.780
O	2.980	10.950	5.602	1.611	3.141
HT	4.048	10.860	12.320	1.611	5.821

Table IV.   Analysis of the Profilometer-Based Sq Data

Heat Treatment	Linear Model t-Values		Quadratic Model t-Values		
	A0 (Intercept)	A1	A0 (Intercept)	A1	A2
H32	0.875	1.398	0.020	1.856	−1.464
O	−1.040	9.486	0.605	1.065	2.617
HT	0.311	38.710	1.042	9.356	1.260

Table V.   Analysis of Variance (ANOVA) Results Assuming No Error in Strain

Heat Treatment	Data Source	ANOVA P-Value	Significant Improvement with Quadratic Fit?
H32	confocal	0.517	no
O	confocal	0.026	yes
HT	confocal	0.004	yes
H32	profiles	0.281	no
O	profiles	0.047	marginal
HT	profiles	0.801	no

the relative error in Y is at least one order of magnitude greater than the relative error in X.

As shown in Table II, the relative standard uncertainty of the means of the strain values ranges between 0.4 and 4.7 pct relative error (RE). In addition, some of the error values lie in the 1 to 3 pct range, and none of the data exhibit a clear, consistent pattern of increase or decrease as a function of strain. Recalling that Sq is one standard deviation of the superposed height distribution, one can use a propagation-of-error approximation to estimate the RE in Sq (*i.e.*, $\text{RE} = \left(\frac{(Sq/\sqrt{2n})}{s} \right) \times 100$, where n is the sample size upon which the standard deviation is based). This expression reveals that the RE is 0.25 pct for the Sq_{prof} data and 0.06 pct for the Sq_{slcm}

**The relative error in the Sq data was substantially reduced by the superposition of the five individual data sets into a single distribution. If the data were not superposed, the mean relative error would be $\cong 0.56$ pct for the Sq_{prof} data and $\cong 0.14$ pct for the Sq_{slcm} data.

---

data.** Both Sq relative error values are considerably smaller than the relative error in the strain data. As such, reversing the X-Y orders of magnitude is required for OLS.

There are two standard approaches to regression analysis in situations where the error magnitudes are reversed (*i.e.*, $RE(X) > RE(Y)$). The first method is to simply reverse the roles of X and Y variables. That is, model the strain as a linear, or curvilinear, function of Sq. Even though the order of magnitude rule may not consistently hold for the Sq_{prof} data, it does hold for the Sq_{slcm} data, and in all cases, $RE(\text{strain}) > RE(Sq)$. Consequently, the error structure of the reversed X and Y data is in better accord with the OLS assumption, and one can apply the standard model ANOVA comparison.

The ANOVA on the Sq_{prof} HT data produces a clear preference for the linear model with either variable ordering ($P = 0.80$ for X-Y compared to $P = 0.72$ for Y-X), whereas the Sq_{slcm} HT data exhibit a borderline to strong preference for the quadratic model ($P = 0.004$ for X-Y compared to $P = 0.054$ for Y-X). In the case of the H32 data, both variable orderings support a linear model for the Sq_{prof} data ($P = 0.28$ for X-Y compared to $P = 0.13$ for Y-X). Similar results were obtained for the Sq_{slcm} data ($P = 0.52$ for X-Y compared to $P = 0.89$ for Y-X). The most significant variable ordering difference was observed in the O condition. The Sq_{prof} data exhibit a borderline quadratic preference

($P = 0.047$) for X-Y, but a strongly quadratic preference ($P = 0.001$) for Y-X. In contrast, the Sq_{slcm} data exhibit a strong quadratic preference for X-Y, but a strong linear preference for Y-X. Even though the trends were reversed for the O condition, the similarities observed in the trends for the HT and the H32 heat treatments indicate that reversing the order of the strain and Sq variables produced comparatively consistent results.

A second standard approach to regression when the error magnitudes are reversed is to apply Errors in Variables methodology.[31] Since an exact, closed-form theory for a specific nonstandard case (*e.g.*, when the estimated standard errors fluctuate in a haphazard manner, such as that exhibited by the strain data) can be difficult to implement, one approach is to use orthogonal distance regression (ODR). ODR employs an optimization algorithm that estimates the polynomial coefficients by minimizing the squared sums of the X and Y errors together, whereas OLS only minimizes the errors in the Y variable.

Many software packages include ODR analysis. The results presented here are derived from the ODRPACK adaptation available in DATAPLOT.[†][32] Analyses of

---

†Dataplot is a free, downloadable statistical software package maintained by the National Institute of Standards and Technology. Additional information about this package can be obtained at the Dataplot web page.

---

the t-statistics of the ODR coefficients along with the magnitudes of the residual standard error revealed the following. In the HT condition, a no-intercept linear model was more appropriate for the Sq_{prof} data, whereas a quadratic model was more appropriate for the Sq_{slcm} data. In the H32 condition, a quadratic was the more appropriate model for the Sq_{prof} data, which contradicts both sets of OLS results. The ODR results were consistent with the OLS results for the Sq_{slcm} data in that a linear model was more appropriate. As was the case with the reversed OLS results, the ODR results for the O condition were less obvious. A quadratic model was slightly more appropriate for the Sq_{prof} data, whereas neither model was clearly dominant in the Sq_{slcm} data. Table VI is a summary of the most appropriate model as determined by each of the three regression analyses.

Regardless of the regression method used, the most obvious difference in the form of the regression model for

Table VI. Summary of the Regression Analyses Results

Heat Treatment	Data Source	Ordinary Least-Squares Regression (OLS)	Reversed Ordinary Least-Squares Regression (r-OLS)	Orthogonal Direction Regression (ODR)
H32	confocal	linear	linear	linear
O	confocal	quadratic	linear	ambiguous
HT	confocal	quadratic	ambiguous	quadratic
H32	profiles	linear	linear	quadratic
O	profiles	ambiguous	quadratic	quadratic
HT	profiles	linear	linear	linear

(a) Profile Data Linear Model

(b) Profile Data Quadratic Model

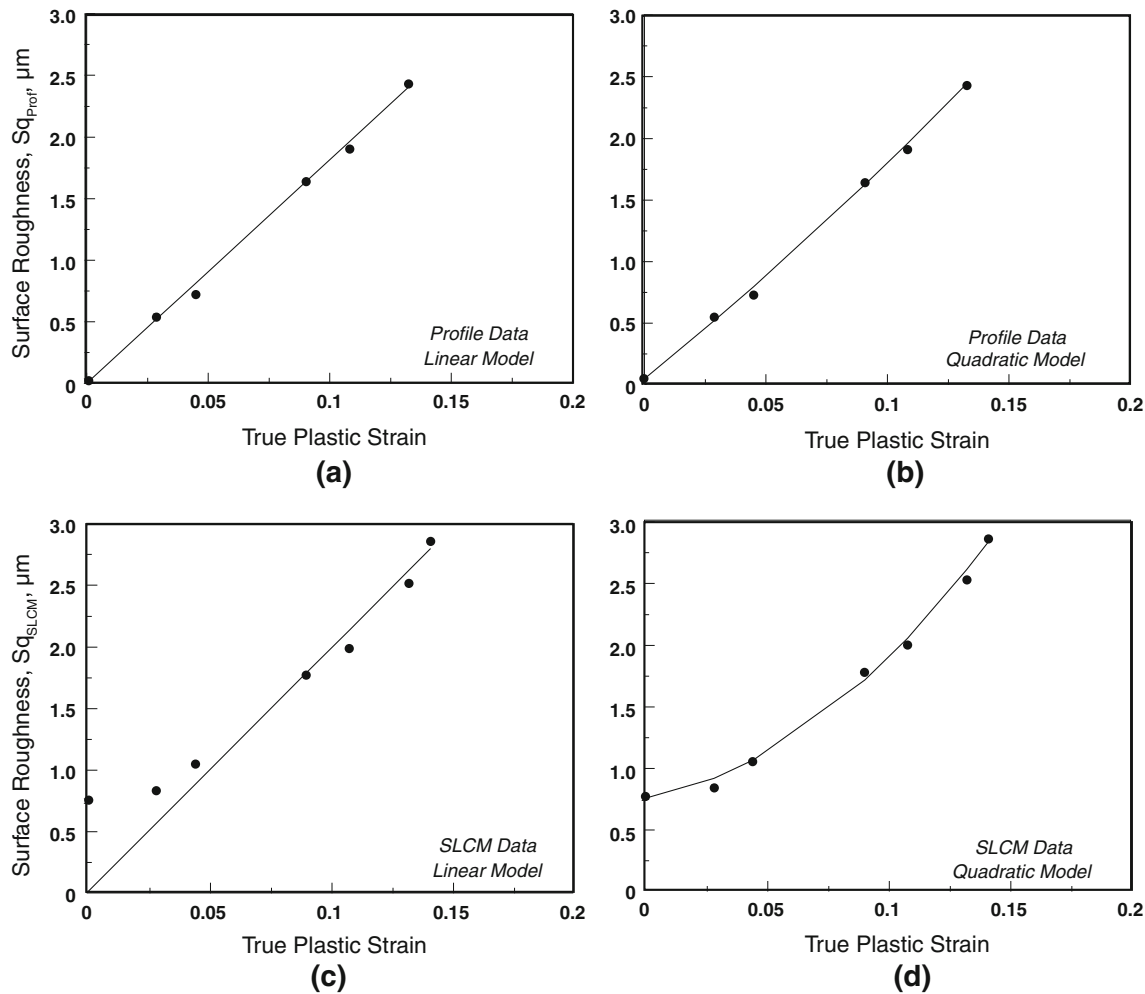**(c)** SLCM Data Linear Model

(d) SLCM Data Quadratic Model

Fig. 5—The best linear and quadratic models shown in individual plots of Sq *vs* true plastic strain using both the contact profilometry and the scanning laser confocal microscope data sets. The difference in the preference for a particular model is graphically obvious for each data set.

IV. DISCUSSION OF RESULTS

the Sq data was observed in the HT heat treatment. This difference is illustrated for the two acquisition techniques in Figure 5. In this figure, the best linear and quadratic models are plotted as Sq *vs* true plastic strain using the Sq_{prof} and Sq_{slcm} data sets. The preference for a particular model is graphically obvious for each data set.

The differences in the results of the regression analyses raise two fundamental questions: Which data set provides the better representation of the true relationship between Sq and plastic strain, and why does the regression model change from linear to quadratic as a function of the grain size?

The answer to the first question lies in the manner in which the surface data are sampled. The stylus profilometry technique has many associated issues that could influence the quality of the surface data. The most germane to this evaluation is mechanical filtering. Even though great care was exercised during the acquisition of the profile data, natural filtering of the surface data in a way that alters the magnitudes of profile characteristics
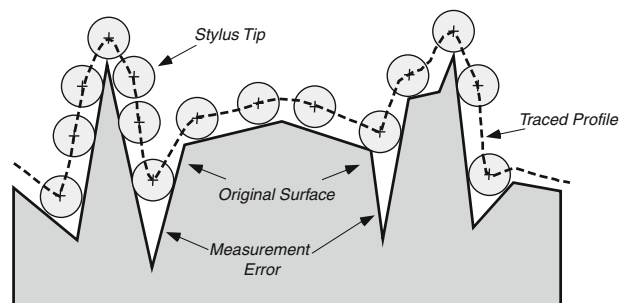

Fig. 6—A schematic showing how the size ratio between the profile tip and the surface features could adversely influence the accuracy of a contact profilometer measurement.[33] Such filtering would tend to artificially skew the roughness data toward the component(s) that produce the largest surface displacements (*i.e.*, grain boundary–localized roughness).

(*i.e.*, the peaks and valley values) is unavoidable in any contact technique. Radhakrishnan[33] showed how the size ratio between the profile tip and the surface features could adversely influence the accuracy of the profilometer measurement. As shown schematically in Figure 6,

mechanical filtering tends to distort the true character of the topography data by artificially accentuating the shear magnitudes of the peaks, reducing the magnitudes of the valleys, and suppressing the contributions to the magnitude of Sq by the more subtle features in the profile. The resulting bias in the surface measurement could easily degrade the fidelity to the point where the only possible outcome is the simplest relationship between Sq and plastic strain.

The SLCM data are not mechanically filtered, because they are derived from a noncontact optical technique. Furthermore, the technique developed to extract and evaluate the surface data from the topographical images captures a higher degree of the three-dimensional character of the surface features. This results in a more accurate representation of the original surface than that provided by the profilometer data. The basis for this assertion is the combination of a smaller probe (635 nm) and the aforementioned spacing between the measured surface heights in each of the five SLCM images. Recall that the spacing between points was 1.56 μm in both the x- and y-directions and encompassed an image area of 6.4×10^5 μm^2. While the 0.22 μm/point spacing in the profilometer data is better than the SLCM in the x-direction, the offset between the 10 profilometer traces (the y-direction) was approximately 1 mm. That is, a four orders of magnitude improvement in the sensitivity of the sampling in the y-direction achieved through SLCM enables a substantially more robust statistical analysis of the surface data. Areal scans are certainly possible with profilometry; however, this approach was not practical in this situation for two reasons. First, the traces cannot be closer than the radius of the profile tip, which in this case is 5 μm and is at least 3 times greater than the distance in the SLCM. Second, an additional offset must be included to compensate for the surface that is destroyed by the ceramic tip during the acquisition of the data. The combination of the higher density of samples in the SLCM data and the lack of mechanical filtering provides substantially greater surface detail than the profile data ($\approx 1.3 \times 10^6$ samples/strain condition $vs \approx 80 \times 10^3$ samples/strain condition). As a result, the same level of surface detail is simply not obtainable with profilometry under these conditions. Therefore, despite the presence of a small offset at zero strain, the trends exhibited by the SLCM data are considered the better representation of the true relationships between Sq and plastic strain for this evaluation.

The composition of the data in the sample is the key to the answer for the second question, why does the regression model change with grain size. Plastic deformation in a polycrystal occurs by a highly complex process, and the measurable surface roughness is generally composed of two types: within-grain roughness and grain boundary–localized roughness. The amount of deformation that occurs within each grain depends on several factors: the orientation and the Taylor factor[34] of the individual grains, and the constraints imposed by neighboring grains at or below the surface. That is, for a grain in a favorable orientation for slip, the deformation will occur by primary slip in the interior regions of that grain. However, in a grain where the slip conditions are not as favorable, the deformation will localize in the grain boundary regions due to the additional shear displacements required to produce grain rotation and to maintain grain-to-grain contiguity.[35] The resulting grain-to-grain anisotropy produces an overall roughness character that is a mixture of both primary slip and near grain boundary deformation. Moreover, neighboring surface grains possessing the same level of macroscopic strain can exhibit appreciably different amounts of measurable surface roughness.[6] Since the anisotropy is strongly influenced by the number of grains in a particular sample, the grain size becomes a critical factor in the deformation process. In fact, the component that has the greatest influence on the magnitude of the surface roughness in a polycrystal is the roughening resulting from the grain-to-grain anisotropy. This is also referred to as grain boundary–localized roughness.

An example of how grain size effects can influence the relationship between plastic strain and the character of the deformed surface is shown in Figure 7. The three topographies in the figure were all acquired at the same magnification after the application of approximately 0.1 true uniaxial strain. As shown in Figure 7(a), the fine grain size in the H32 condition produces a high number of grain boundaries per unit area. Since the surface data in this condition consist almost entirely of grain boundary–localized surface roughness, the Sq_{slcm} values primarily reflect the influence of that component. This is exhibited in the relationship between Sq_{slcm} and plastic strain, which was linear for all the regression methods. As the grain size increases (Figures 7(b) and (c)), the area fraction of grain boundaries decreases and the ratio of grain boundary–localized roughness to within-grain roughness changes accordingly. The corresponding relationship between Sq and plastic strain also becomes more curvilinear in nature. The surface morphology of the largest grain size (HT, Figure 7(c)) is distinctly different from that exhibited in the H32 heat treatment (Figure 7(a)) at the same strain level. The relative fraction of within-grain roughness in the figure is substantially higher than the grain boundary–localized roughness, and this produces a more complex relationship between Sq_{slcm} and plastic strain for the HT heat treatment. Note that these results are based on images acquired with a 10 times objective lens. If the SLCM data were acquired at a different magnification, the relative ratios of grain-boundary–localized to within-grain roughness, as well as the relationship between Sq_{slcm} and plastic strain exhibited in the H32 data, are likely to be considerably different.

The composition of the surface data is not the sole basis for the change in regression model with grain size. It was the analysis technique that we developed,[15] which superposes the individual topographic samples into a large single distribution and subsequently minimizes the associated statistical uncertainty in Sq that revealed the subtle influences of the composition on the character of the surface roughness. This influence is obscured in the profilometry data by the aforementioned lack of sampling sensitivity in the x-y plane. As a result, the regression analyses do not indicate any discernable trend between Sq_{prof}, plastic strain, and grain size.

Tensile Axis

(a) H32 Condition

100 µm

(b) O Condition

100 µm

(c) HT Condition

100 µm

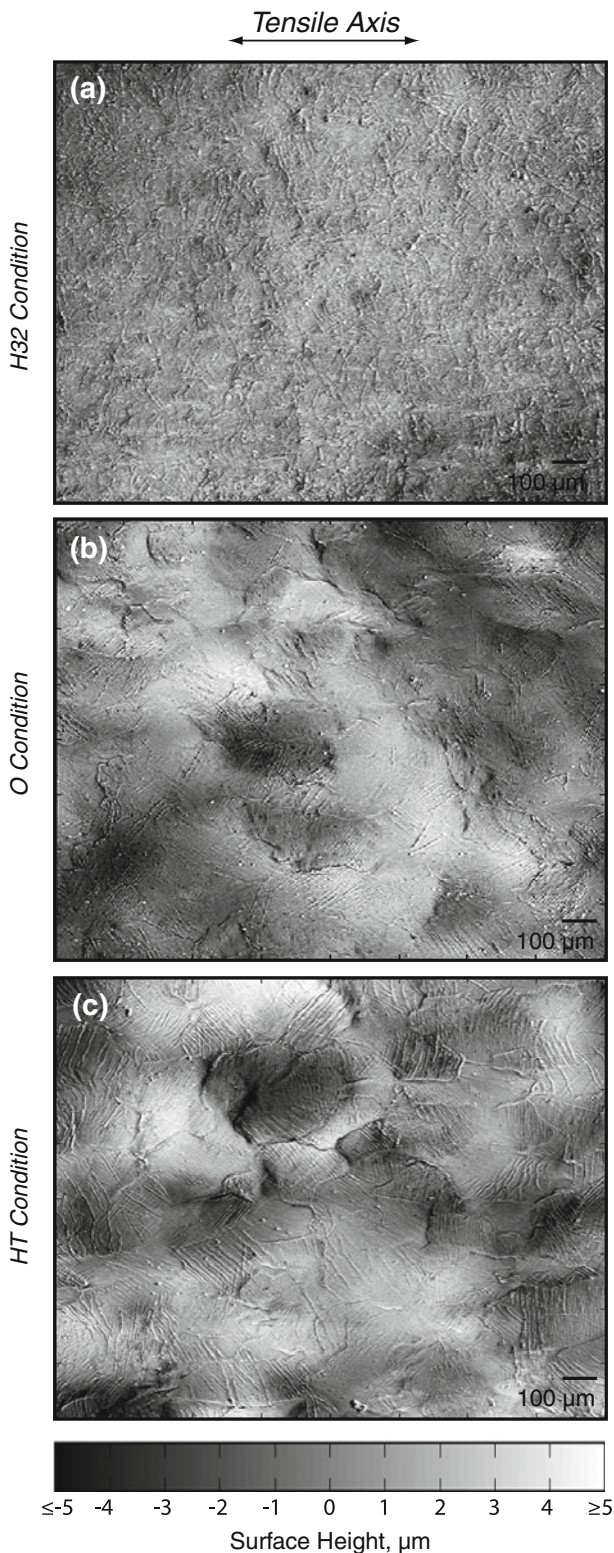≤-5 -4 -3 -2 -1 0 1 2 3 4 ≥5
Surface Height, µm

Fig. 7—An example of how the grain size influences the composition of surface roughness data. The three topographies shown in this figure were all acquired at the same magnification after approximately 0.1 true uniaxial strain. The ratio of grain boundary roughness and slip-induced roughness changes with increasing grain size in these figures. Similarly, the composition of the surface roughness in the HT condition (C) is distinctly different for that in the H32 condition (A).

Because the SLCM data capture more of the influence of the composition on the roughness, these measurements appear to produce the more reliable trends.

V. CONCLUSIONS

Three different heat treatments of AA5052 were subjected to various levels of uniaxial plastic strain, and the resulting surfaces were evaluated using two different data acquisition techniques: SLCM and stylus profilometry. The behaviors of the surface data from both sources were analyzed using a technique that minimizes the statistical uncertainty in the Sq data and compared as a function of true plastic strain. The trends in the Sq data were then evaluated with three different statistical methods to determine the more appropriate regression model for the relationship between the Sq data and true plastic strain. The first method was a standard OLS and model comparison ANOVA. The magnitudes of the error in the strain were found to be substantially larger than that in the Sq data. The roles of the X and Y variables were then reversed and a second OLS/ANOVA was performed on those data. The third method, ODR, which simultaneously accounts for the error in both the strain and Sq data, was also employed. Even though the sizes of the available data sets did cause some differences among the results from the different regression methods, these analyses demonstrated that a linear fit was statistically more appropriate for the finest grain size (the H32 heat treatment) and that, as the grain size increased, a quadratic fit became the better statistical model. The ANOVA performed on the profilometry data did not reveal any discernable trends.

The differences observed between the SLCM and the profilometry behaviors were attributed to two sources: the manner in which the surface data were sampled and the composition of the data in the surface measurements. The mechanical filtering inherent to the contact profilometry technique introduced a bias that degraded the fidelity of the surface data and altered the relationship between Sq and plastic strain. In contrast, the SLCM data are not mechanically filtered and the technique developed to extract and evaluate the surface data from sets of topographical images captured more of the three-dimensional character of the surface features. The higher density of surface samples in the SLCM measurements produced a more robust representation of the original surface than the profilometer measurements. Therefore, even though a small offset was observed in the SLCM data at zero strain, the trends exhibited by these data are considered the more reliable representation of the true relationships between Sq and plastic strain for this evaluation.

The composition of the topographic data in these analyses changed because the relative area fractions of grain boundary–localized roughness and within-grain roughness are both dependent on the grain size. The fine grain size produced a more linear relationship between Sq and plastic strain, because the topographies consist almost entirely of grain boundary–localized roughness.

That is, the measurable roughness is primarily influenced by a single component that generally scales linearly with strain. An increase in grain size reduced the relative area fraction of grain boundaries, thereby altering the ratio between grain boundary roughness and within-grain roughness. This was illustrated in a side-by-side comparison of the topographies produced by 10 pct true uniaxial strain. The complex surface morphology in the largest grain size required a more complex relationship between Sq and plastic strain to describe the behavior.

The answer to the question of whether the relationship between surface roughness and plastic strain is truly linear seems to be "it depends." Considering all of the factors that could influence the composition or the interpretation of surface roughness data in any given measurement, *a priori* assumptions regarding the form of the relationship that exists between surface roughness and plastic strain are simply not appropriate. Such assumptions become particularly precarious when the character of the surface roughness data is a key factor in a numerical model designed to predict the behavior during sheet metal forming.

REFERENCES

1. W.K. Liu, L. Siad, R. Tian, S. Lee, D. Lee, X.L. Yin, W. Chen, S. Chan, G.B. Olson, L.E. Lindgen, M.F. Horstemeyer, Y.S. Chang, J.B. Choi, and Y.J. Kim: *Int. J. Numer. Methods Eng.*, 2009, vol. 80, pp. 932–78.
2. K. Thornton, S. Nola, R.E. Garcia, M. Asta, and G.B. Olson: *JOM*, 2009, vol. 61, pp. 12–17.
3. T.V. Vorburger, H.G. Rhee, T.B. Renegar, J.F. Song, and A. Zheng: *Int. J. Adv. Manufact. Technol.*, 2007, vol. 33, pp. 110–18.
4. H. Rhee, T.V. Vorburger, J.W. Lee, and J. Fu: *Appl. Optics*, 2005, vol. 44, pp. 5919–27.
5. J.S. Bendat and A.G. Piersol: *Random Data—Analysis and Measurement Procedures*, John Wiley & Sons, New York, NY, 1986, pp. 1–566.
6. M.R. Stoudt and J.B. Hubbard: *Acta Mater.*, 2005, vol. 53, pp. 4293–4304.
7. M.R. Stoudt and R.E. Ricker: *Metall. Mater. Trans. A*, 2002, vol. 33A, pp. 2883–89.
8. W.R.D. Wilson and W. Lee: *J. Manuf. Sci. Eng.*, 2001, vol. 123, pp. 279–83.
9. I. Shimizu, T. Okuda, T. Abe, and H. Tani: *JSME Int. J. A*, 2001, vol. 44, pp. 499–506.
10. Y.Z. Dai and F.P. Chiang: *J. Eng. Mater. Technol.*, 1992, vol. 114, pp. 432–38.
11. N. Kawai, T. Nakamura, and Y. Ukai: *Bull. JSME*, 1986, vol. 29, pp. 1337–43.
12. T. Abe, S. Nagaki, and T. Akase: *Bull. JSME*, 1985, vol. 28, pp. 251–58.
13. K. Osakada and M. Oyane: *Bull. JSME*, 1971, vol. 14, pp. 171–77.
14. A. Perron, O. Politano, and V. Vignal: *Surf. Interface Anal.*, 2008, vol. 40, pp. 518–21.
15. M.R. Stoudt, J.B. Hubbard, and S.A. Janet: *Mater. Sci. Technol.*, 2008, vol. 24, pp. 253–60.
16. P.D. Wu and D.J. Lloyd: *Acta Mater.*, 2004, vol. 52, pp. 1785–98.
17. U. Borg and N.A. Fleck: *Strain Gradient Effects in Surface Roughening*, Iop Publishing Ltd, Bristol, United Kingdom, 2007, pp. S1–S12.
18. Anon.: *Aluminum Standards and Data 2003*, The Aluminum Association, Washington, DC, 2003, pp. 1–235.
19. Anon.: *2000 Annual Book of ASTM Standards, Section 3, Metals Test Methods and Analytical Procedures*, ed., ASTM, Philadelphia, PA, 2000, pp. 240–63.
20. G.F. VanderVoort: *Metallography Principles and Practice*, ASM INTERNATIONAL, Materials Park, OH, 1999, pp. 1–752.
21. M.R. Stoudt, J.B. Hubbard, M.A. Iadicola, and S.W. Banovic: *Metall. Mater. Trans. A*, 2009, vol. 40A, pp. 1611–22.
22. M.R. Stoudt, J.B. Hubbard, S.P. Mates, and D.E. Green: *SAE Trans. J. Mater. Manufact.*, 2006, vols. 114–115, pp. 183–90.
23. Anon.: *ASME Designation B46.1-2002: Surface Texture (Surface Roughness, Waviness and Lay)*, ASME, New York, NY, 2002, pp. 1–98.
24. T.R. Thomas: *Rough Surfaces*, Imperial College Press, London, 1999, pp. 1–278.
25. W. Chu, J. Fu, R. Dixson, G. Orji, and T. Vorburger: *Rev. Sci. Instrum.*, 2009, vol. 80. DOI:07370910.1063/1.3189041.
26. J. Song, T. Vorburger, T. Renegar, H. Rhee, A. Zheng, L. Ma, J. Libert, S. Ballou, B. Bachrach, and K. Bogart: *Meas. Sci. Technol.*, 2006, vol. 17, pp. 500–03.
27. L.C. Hamilton: *Regression with Graphics: A Second Course in Applied Statistics*, Brooks/Cole Publishing Company, Pacific Grove, CA, 1992, pp. 1–363.
28. Anon.: *F-Test*, Wikipedia, The Free Encyclopedia, 2009.
29. R.E. Walpole and R.H. Myers: *Probability and Statistics for Engineers and Scientists*, The Macmillan Co., New York, NY, 1972, pp. 1–506.
30. M.J. Crawley: *Statistical Computing: An Introduction to Data Analysis Using S-Plus*, John Wiley & Sons, New York, NY, 2002, pp. 1–761.
31. W. Fuller: *Measurement Error Models*, John Wiley, New York, NY, 1987, pp. 1–440.
32. J. Filliben and N.A. Heckert: *Dataplot*, NIST, Gaithersburg, MD, 1978.
33. V. Radhakrishnan: *Wear*, 1970, vol. 16, pp. 325–35.
34. G.I. Taylor: *J. Inst. Met.*, 1938, vol. 62, pp. 307–24.
35. M.F. Ashby: *Phil. Mag.*, 1970, vol. 21, pp. 399–424.